

## NUCLEOSYNTHESIS OF RARE NUCLEI FROM SEED NUCLEI IN EXPLOSIVE CARBON BURNING\*

W. MICHAEL HOWARD,<sup>†</sup> W. DAVID ARNETT,<sup>‡</sup> DONALD D. CLAYTON,  
AND STANFORD E. WOOSLEY

Rice University, Houston, Texas, and Institute of Theoretical Astronomy, Cambridge, England

*Received 1971 December 10*

### ABSTRACT

We demonstrate that a Population I concentration of primordial heavy seed nuclei, when present in the carbon- and oxygen-rich core of the presupernova star and exposed to the temperature and free nucleon densities of explosive carbon burning, is efficiently transmuted into the rare species  $^{36}\text{S}$ ,  $^{40}\text{K}$ ,  $^{40}\text{Ar}$ ,  $^{43}\text{Ca}$ ,  $^{46}\text{Ca}$ ,  $^{48}\text{Ca}$ ,  $^{45}\text{Sc}$ ,  $^{47}\text{Ti}$ ,  $^{49}\text{Ti}$ ,  $^{50}\text{Ti}$ ,  $^{50}\text{V}$ ,  $^{62}\text{Ni}$ ,  $^{64}\text{Ni}$ ,  $^{68}\text{Zn}$ ,  $^{70}\text{Zn}$ , and  $^{76}\text{Ge}$  in approximately their solar-system abundance ratios. If the temperature is high enough ( $T_9 \simeq 2.1$ ) that at least 10 percent of the Fe and Ni seed nuclei undergo  $(p, n)$  reactions during the explosion, the nuclei  $^{65}\text{Cu}$ ,  $^{67}\text{Zn}$ ,  $^{71}\text{Ga}$ ,  $^{73}\text{Ge}$ , and perhaps  $^{76}\text{As}$  can also be synthesized. These nuclei comprise virtually all of the relatively rare neutron-rich nuclei in the range  $36 \leq A \leq 76$  except  $^{54}\text{Cr}$  and  $^{58}\text{Fe}$ . We emphasize the dependence of the results upon the rates of important nuclear reactions, most of which are unknown. The temperature, density, and timescale of the carbon explosion all have a strong influence on the results as well. We therefore regard this paper as an exploratory survey of a very difficult problem that will give increasing information about nucleosynthesis as nuclear facts and models of nuclear explosions become more secure.

### I. INTRODUCTION

The features of the solar-system abundance distribution (including isotopic abundance ratios) of the elements can be produced with a remarkable degree of success by calculating the nucleosynthesis that takes place when massive stars burn their evolved cores and outer layers violently and quickly on a hydrodynamic timescale (see the recent review by Arnett and Clayton 1970). In particular, the explosive burning of  $^{12}\text{C}$  (Arnett 1969) in zones that have undergone hydrostatic helium burning seems to synthesize the solar-system abundance distribution of  $^{20}\text{Ne}$ ,  $^{23}\text{Na}$ ,  $^{24,25,26}\text{Mg}$ ,  $^{27}\text{Al}$ ,  $^{29,30}\text{Si}$ , and  $^{31}\text{P}$ . At higher temperatures the explosive burning of  $^{16}\text{O}$  (Truran and Arnett 1970; Woosley, Arnett, and Clayton 1972) in zones that have completed hydrostatic carbon burning may account for the solar-system abundance of  $^{28}\text{Si}$  and for abundances of major nuclei in the mass range  $32 \leq A \leq 42$ . The abundances of  $^{46}\text{Ti}$  and  $^{50}\text{Cr}$  are also produced in this calculation. Recent calculations (Arnett, Truran, and Woosley 1971; Woosley *et al.* 1972) show that explosive burning at even higher temperatures merges into quasi-equilibrium abundances (Bodansky, Clayton, and Fowler 1968) slightly altered by the cooling of the gas and by electron-capture to produce nuclei in the mass range of the iron group ( $48 \leq A \leq 62$ ).

In spite of this overwhelming success, many rare nuclei in the designated mass ranges are not produced by the explosive fuels. In particular, the relatively rare neutron-rich nuclei  $^{36}\text{S}$ ,  $^{40}\text{Ar}$ ,  $^{40}\text{K}$ ,  $^{43}\text{Ca}$ ,  $^{46}\text{Ca}$ ,  $^{48}\text{Ca}$ ,  $^{45}\text{Sc}$ ,  $^{47}\text{Ti}$ ,  $^{49}\text{Ti}$ ,  $^{50}\text{Ti}$ ,  $^{50}\text{V}$ ,  $^{54}\text{Cr}$ ,  $^{58}\text{Fe}$ ,  $^{63}\text{Cu}$ ,  $^{65}\text{Cu}$ ,  $^{64}\text{Ni}$ ,  $^{66}\text{Zn}$ ,  $^{68}\text{Zn}$ , and  $^{70}\text{Zn}$  are not, with possible exceptions of  $^{45}\text{Sc}$  and  $^{49}\text{Ti}$ , synthesized in the above-mentioned calculations. To have a consistent and viable understanding of the thermonuclear origin of the elements we must account for all nuclear species in the

\* Work supported in part by the National Science Foundation grants GP-18335 and GP-23459.

<sup>†</sup> Present address: Los Alamos Scientific Laboratory, Los Alamos, New Mexico.

<sup>‡</sup> Alfred P. Sloan Foundation Fellow. Present address: Departments of Astronomy and Physics, University of Texas, Austin, Texas 78712.

applicable mass range. Although almost all of the above-mentioned nuclei are rare, it seems important to us to account for their existence. We will report in this paper on a possible source of these nuclei that is a direct result of the explosive burning of carbon.

We assume that the presupernova star formed from material of solar-system composition, taking with minor modifications the abundances of Cameron (1968). The abundances of  $^{36}\text{Ar}$  and  $^{38}\text{Ar}$  have been reduced a factor of 2 from Cameron's value to account for recent results from lunar samples analyzed by Eberhardt *et al.* (1970), and the numerical abundance  $^{40}\text{K} = 4.3$  per  $10^6$  silicon atoms is taken as the abundance when the Sun formed. The star is then initially composed of approximately 0.27 percent by mass of nuclei heavier than Mg. This mass is primarily in the form of  $^{58}\text{Ni}$ ,  $^{60}\text{Ni}$ ,  $^{54}\text{Fe}$ ,  $^{56}\text{Fe}$ ,  $^{57}\text{Fe}$ ,  $^{52}\text{Cr}$ ,  $^{40}\text{Ca}$ ,  $^{36}\text{Ar}$ ,  $^{38}\text{Ar}$ ,  $^{32}\text{S}$ ,  $^{34}\text{S}$ ,  $^{31}\text{P}$ ,  $^{28}\text{Si}$ ,  $^{29}\text{Si}$ , and  $^{30}\text{Si}$ , which are those nuclei having mass fractions  $X > 10^{-5}$  g g $^{-1}$ . We assume that these nuclei remain unaltered during the hydrostatic evolution of the star and act as "seed" for the free protons, neutrons, and  $\alpha$ -particles liberated in the explosive carbon-burning shell. Although the concentration of these seed nuclei is small compared to that of the  $^{12}\text{C}$  and  $^{16}\text{O}$  in the shell, the solar mass fractions of the rare neutron-rich nuclei are even smaller (typically  $10^{-7} < X < 10^{-8}$ ). The seed abundances are sufficiently small that they consume only a small fraction of the liberated free particles during the explosive carbon burning. We have performed the explosive calculation with and without the seed nuclei as neutron absorbers, for example, and have found a negligibly small change in the free neutron density. We have therefore taken the free-particle densities as a function of time directly from explosive-carbon-burning calculations. This is a great simplification which allows us to decouple the fate of the seed nuclei from the small perturbation they make in the carbon burning.

## II. METHOD OF CALCULATION

A computer code follows the abundance changes of the seed nuclei due to nuclear interactions when it is given the free-particle densities and the temperature as a function of time. The system of equations is linear in the sense that if each initial seed nucleus is multiplied by a factor  $\alpha$ , the final abundances are multiplied by the same factor  $\alpha$ . The dependence on the free-nucleon densities is more complicated. Interactions with  $\alpha$ -particles can be ignored. As in previous explosive nucleosynthesis calculations, the density is taken to decrease one  $e$ -fold on a hydrodynamic timescale taken to be  $\tau_\rho = (24\pi G\rho_0)^{-1/2}$ , and the expansion is taken to be adiabatic so that  $\rho \propto T^3$  is a good approximation. The network for calculating the fate of the seed nuclei in the charge region  $12 \leq Z \leq 24$  involves as many as 91 species, including the isotopes  $^{28}\text{Si}$  through  $^{35}\text{Si}$ ,  $^{30}\text{P}$  through  $^{36}\text{P}$ ,  $^{32}\text{S}$  through  $^{37}\text{S}$ ,  $^{35}\text{Cl}$  through  $^{46}\text{Cl}$ ,  $^{36}\text{Ar}$  through  $^{47}\text{Ar}$ ,  $^{39}\text{K}$  through  $^{50}\text{K}$ ,  $^{40}\text{Ca}$  through  $^{51}\text{Ca}$ ,  $^{43}\text{Sc}$  through  $^{50}\text{Sc}$ ,  $^{45}\text{Ti}$  through  $^{51}\text{Ti}$ ,  $^{47}\text{V}$  through  $^{51}\text{V}$ , and  $^{48}\text{Cr}$  through  $^{51}\text{Cr}$ . The limits on the size of the network were chosen from considerations of neutron separation energies for neutron-rich nuclei and of the rates for the charge-increasing ( $p, \gamma$ ) and ( $p, n$ ) reactions for the neutron-rich nuclei. The calculations of reactions on Fe and Ni seed nuclei were performed considering only ( $n, \gamma$ ) and ( $\gamma, n$ ) reactions. At the temperatures we are considering ( $1.8 \leq T_9 \leq 2.15$ ), we can ignore proton-induced reactions for  $Z > 26$  with an important exception to be mentioned later, and ( $n, p$ ) and ( $n, \alpha$ ) reactions are energetically highly unfavorable. The Cr seed nuclei are not significant sources for any product.

A differential equation for the rate of change of the number density of each nuclear species is written involving the participating reaction rates. The set of linear differential equations are then solved by a method of backward differencing at each time, as described by Arnett and Truran (1969). Experimental rates for charged-particle-induced reactions, when available, were taken from Fowler, Caughlan, and Zimmerman (1971). The rates of Allen, Gibbons, and Macklin (1971) served as guides to these reactions and were extrapolated to the required temperature. Estimated rates were provided by Truran (1971); experimental binding energies were used when possible, but unmeasured

values were taken from estimates by Garvey *et al.* (1969). Beta-decay rates from the ground state of radioactive nuclei were found to play no role in the nuclear processing and were not included.

In table 1 we list the important reactions and the values of their rates for two values of the temperature. For particle-induced reactions, we list the product  $N_A \langle \sigma v \rangle$  in cgs units, where  $N_A$  is Avogadro's number. For  $(\gamma, n)$  reactions the entry is the inverse mean lifetime in seconds of the species. The mean lifetime in seconds of the target species against a specific proton-induced reaction, for example, is given by

$$\tau_p = [\rho X_p N_A \langle \sigma v \rangle]^{-1},$$

where  $\rho$  is the total mass density (near  $10^5 \text{ g cm}^{-3}$  in these calculations) and  $X_p$  is the fraction of the mass in the form of free protons (near  $10^{-9}$  in these calculations). This long list of rates should be very helpful not only in understanding what we have done but also in providing a quick estimate of lifetimes near  $T_9 = 2$  for other workers. Examination of this table will in itself show the discerning reader how the flows go in this problem. We do not, however, wish to suggest that these entries are well-established numbers. The footnotes to the table reveal the sources of these numbers, and there the reader will see that many numbers were almost arbitrary choices on our part, especially where we believed the value of the rate to have little influence on the answers. For every reaction listed, the inverse reaction was also in the network. Reactions not listed in table 1 are believed to be unimportant for this problem. An exception to this principle lies in repeated values of cross-sections, which are indicated by the reference notes to the table; for example, the  $(p, n)$  reactions on all unstable neutron-rich isotopes of Cl were taken to have the same cross-section, as indicated by reference note (7) to table 1. Because the event is  $r$ -process-like above Fe, we have not listed the values of  $N_A \langle \sigma v \rangle$  for the  $(n, \gamma)$  reactions on isotopes of Fe, Co, Ni, Cu, and Zn. We actually used the values  $1.9 \times 10^6$ ,  $4.3 \times 10^6$ , and  $1.0 \times 10^7$  for their even-even, even-odd, and odd-odd nuclear isotopes, but the final yields are rather insensitive to the values chosen. Much more important are their  $(\gamma, n)$  rates, which we do list and which are primarily determined by the unknown values of neutron separation energies. Such a rudimentary representation of the nuclear rates is not adequate for accurate solution of this problem; however, it will suffice for these exploratory calculations of what must be an important system of reactions if, in fact, explosive carbon burning actually occurs in nature as a major source of  $^{24}\text{Mg}$  nuclei. Nonetheless, none of the yields we calculate can be regarded as correct to better than a factor of 2 or 3 at best except for specific fortuitous cases. What we will provide is a reliable overview of the general possibilities, and the very encouraging nature of our results more than warrants this approach. It will take many hard years of research into nuclear facts to secure the detailed numerical accuracy.

### III. RESULTS

#### a) Choice of Peak Burning Temperature

The temperature of the carbon burning largely determines the magnitude of the fluxes of free particles. Our basic assumption in this paper will be that the Mg isotopes owe their thermonuclear origin to explosive carbon-burning shells. Recent calculations by one of us (W. D. A.) seem to indicate that the carbon-oxygen-rich shell of a massive ( $M > 10 M_\odot$ ) star will have a density  $\rho \approx 10^5 \text{ g cm}^{-3}$  just prior to its violent disruption. At this density, the peak temperature of the explosive burning must be near  $2 \times 10^9 \text{ K}$  for a significant amount of the  $^{12}\text{C}$  to be transmuted into  $^{20}\text{Ne}$ ,  $^{23}\text{Na}$ ,  $^{24}\text{Mg}$ ,  $^{25}\text{Mg}$ ,  $^{26}\text{Mg}$ ,  $^{27}\text{Al}$ ,  $^{29}\text{Si}$ ,  $^{30}\text{Si}$ , and  $^{31}\text{P}$  in amounts very similar to their solar-system abundance ratios. For  $T_9 < 2$ , less than 10 percent of the carbon burns; and for  $T_9 > 2.2$  the yields of  $^{23}\text{Na}$  and  $^{25,26}\text{Mg}$  become discouragingly small relative to that of  $^{24}\text{Mg}$ . Following this reasoning, we will assume a density  $\rho = 10^5 \text{ g cm}^{-3}$  and calculate the nuclear interac-

TABLE 1. REACTION RATES

Target	Reaction	$N_A < \sigma v >$		Ref <sup>(1)</sup>	Target	Reaction	$N_A < \sigma v >$		Ref <sup>(1)</sup>
		$T_9 = 2.00$	$T_9 = 2.15$				$T_9 = 2.00$	$T_9 = 2.15$	
<sup>32</sup> S	(n, γ) *	4.8 (5)	4.9 (5)		<sup>48</sup> K	(γ, n) *	5.5 (3)	6.7 (4)	(8)
	(n, α)	3.5 (4)	5.0 (4)		<sup>50</sup> K	(γ, n) *	2.1 (8)	1.3 (9)	(8)
<sup>33</sup> S	(n, γ) *!	3.8 (5)	3.8 (5)		<sup>40</sup> Ca	(n, γ) *	1.1 (6)	1.1 (6)	(2)
	(n, α) *!	7.9 (6)	8.6 (6)			(n, p)	2.7 (3)	5.3 (3)	
<sup>34</sup> S	(n, γ) *!	1.1 (5)	1.1 (5)	(2)	<sup>41</sup> Ca	(n, γ) *!	4.2 (6)	4.2 (6)	(2)
<sup>35</sup> S	(n, γ)	3.8 (5)	3.8 (5)	(3)		(n, p) *!	2.1 (6)	2.4 (6)	
	(p, n)	6.3 (4)	9.7 (4)			(n, α) *!	8.1 (6)	8.8 (6)	
<sup>36</sup> S	(n, γ)	5.2 (4)	5.7 (4)	(2)	<sup>42</sup> Ca	(n, γ)	1.2 (6)	1.2 (6)	(2)
	(p, γ) *!	9.7 (3)	1.3 (4)			(p, γ)	7.7 (2)	1.1 (3)	
	(p, n)	1.2 (3)	2.8 (3)		<sup>43</sup> Ca	(n, γ)	1.2 (6)	1.2 (6)	(2)
<sup>37</sup> S	(γ, n)	2.6 (3)	1.9 (4)			(p, γ)	3.1 (3)	4.4 (3)	
<sup>35</sup> Cl	(n, γ)	3.6 (6)	3.7 (6)	(4)	<sup>44</sup> Ca	(n, γ)	2.4 (6)	2.4 (6)	(2)
	(n, p)	2.2 (6)	2.7 (6)			(p, γ)	3.0 (3)	4.4 (3)	
	(p, α)	9.6 (3)	1.4 (4)	(5)	<sup>45</sup> Ca	(n, γ)	3.2 (6)	3.2 (6)	(2)
<sup>36</sup> Cl	(n, γ)	2.2 (6)	2.3 (6)	(6)		(p, n)	1.6 (4)	2.6 (4)	
	(p, n)	3.7 (4)	5.7 (4)		<sup>46</sup> Ca	(n, γ) *	2.4 (6)	2.4 (6)	(2)
	(n, p) *	1.7 (7)	1.8 (7)			(p, γ)	6.5 (3)	1.0 (4)	
	(n, α)	1.3 (5)	1.6 (5)		<sup>47</sup> Ca	(n, γ)	1.8 (6)	1.8 (6)	(2)
<sup>37</sup> Cl	(n, γ) *	4.5 (5)	4.8 (5)	(2)		(p, n) *	1.3 (4)	2.1 (4)	
	(p, n)	3.6 (3)	7.4 (3)		<sup>48</sup> Ca	(n, γ) *	1.2 (5)	1.2 (5)	(2)
	(p, γ) *	3.7 (3)	5.1 (3)	(5)		(p, γ) *	6.6 (3)	1.0 (4)	
	(p, α) *	1.9 (4)	2.6 (4)	(5)	<sup>49</sup> Ca	(n, γ)	6.0 (5)	6.0 (5)	(2)
<sup>38</sup> Cl	(p, n)	3.8 (4)	5.8 (4)	(7)		(γ, n)	1.8 (2)	1.6 (3)	
	(p, α)	8.9 (3)	1.5 (4)			(p, n)	1.3 (4)	2.2 (4)	
<sup>42</sup> Cl	(γ, n)	1.8 (3)	1.9 (4)	(8)	<sup>50</sup> Ca	(n, γ)	6.0 (5)	6.0 (5)	(2)
<sup>44</sup> Cl	(γ, n) *	1.8 (3)	1.9 (4)	(8)	<sup>51</sup> Ca	(γ, n)	9.5 (6)	4.5 (7)	(2)
<sup>46</sup> Cl	(γ, n) *	1.4 (7)	7.8 (7)	(8)	<sup>43</sup> Sc	(n, γ)	1.3 (6)	1.4 (6)	
<sup>36</sup> Ar	(n, γ) *	2.5 (5)	2.7 (5)	(2)		(n, p)	1.3 (8)	1.4 (8)	
	(n, p) *!	2.8 (5)	4.2 (5)			(n, α)	3.6 (4)	4.6 (4)	
	(n, α)	5.3 (4)	7.2 (4)		<sup>44</sup> Sc	(n, γ)	5.8 (6)	6.2 (6)	
<sup>37</sup> Ar	(n, γ)	2.0 (5)	2.1 (5)	(2)		(n, p)	9.5 (7)	1.0 (8)	
	(n, p) *!	3.8 (7)	4.1 (7)			(n, α)	2.2 (5)	2.6 (5)	
	(n, α) *!	1.9 (7)	2.0 (7)			(p, γ)	1.2 (3)	1.8 (3)	
<sup>38</sup> Ar	(n, γ)	7.8 (5)	8.5 (5)	(2)	<sup>45</sup> Sc	(n, γ)	4.1 (6)	4.2 (6)	
	(p, γ) *	1.5 (3)	2.0 (3)			(n, p)	2.6 (5)	3.5 (5)	
<sup>39</sup> Ar	(n, γ)	2.0 (6)	2.1 (6)	(9)		(p, γ)	7.0 (3)	9.6 (3)	(5)
	(p, n)	2.3 (4)	3.6 (4)		<sup>46</sup> Sc	(n, γ)	9.4 (6)	9.5 (6)	
	(n, α)	1.8 (5)	2.2 (5)			(n, p)	1.4 (6)	1.5 (6)	
<sup>40</sup> Ar	(n, γ)	6.7 (5)	7.2 (5)	(10)		(p, n)	4.3 (3)	7.1 (3)	
	(p, n)	4.6 (1)	1.3 (2)			(p, γ)	1.6 (3)	2.6 (3)	
	(p, γ) *	5.1 (3)	7.0 (3)		<sup>47</sup> Sc	(n, γ)	5.6 (6)	6.1 (6)	
<sup>41</sup> Ar	(p, n)	2.9 (4)	4.6 (4)	(11)		(p, n)	7.7 (3)	1.3 (4)	
<sup>43</sup> Ar	(γ, n) *	9.5 (1)	1.1 (3)	(8)	<sup>48</sup> Sc	(n, γ)	1.4 (6)	1.5 (6)	
<sup>45</sup> Ar	(γ, n) *	1.3 (3)	1.3 (4)	(8)		(p, n)	1.2 (3)	2.0 (3)	
<sup>47</sup> Ar	(γ, n) *	9.1 (5)	5.8 (6)	(8)		(p, γ)	1.2 (3)	2.0 (3)	
<sup>39</sup> K	(n, γ) *!	3.5 (6)	3.5 (6)	(2)	<sup>49</sup> Sc	(n, γ)	3.5 (5)	3.7 (5)	
	(n, p)	1.6 (5)	2.3 (5)			(p, n) *	8.3 (3)	1.4 (4)	
	(p, γ)	3.8 (2)	5.4 (2)	(5)	<sup>50</sup> Sc	(γ, n)	2.9 (0)	4.4 (1)	
<sup>40</sup> K	(n, γ)	1.1 (6)	1.1 (6)	(2)		(p, n)	5.8 (4)	9.6 (4)	
	(n, p)	3.1 (6)	3.4 (6)			(p, γ)	2.0 (4)	3.3 (4)	
	(p, n)	6.8 (3)	1.1 (4)		<sup>45</sup> Ti	(n, γ)	8.6 (6)	8.8 (6)	
	(n, α)	2.6 (6)	3.0 (6)			(n, p)	1.7 (8)	1.8 (8)	
<sup>41</sup> K	(n, γ)	2.8 (6)	3.8 (6)			(n, α)	1.5 (8)	1.6 (8)	
	(p, n)	4.0 (3)	7.5 (3)		<sup>46</sup> Ti	(n, γ)	2.0 (6)	2.2 (6)	
	(p, γ)	1.5 (3)	2.0 (3)			(p, γ)	8.1 (2)	1.2 (3)	
	(p, α)	4.1 (3)	6.4 (3)		<sup>47</sup> Ti	(n, γ)	7.4 (6)	7.5 (6)	
<sup>42</sup> K	(n, γ)	1.1 (7)	1.1 (7)	(12)		(n, p)	2.9 (4)	4.5 (4)	
	(n, p)	8.6 (4)	1.3 (5)	(11)		(p, γ)	2.8 (3)	4.3 (3)	
	(p, n)	2.9 (4)	3.0 (4)	(13)	<sup>48</sup> Ti	(n, γ)	1.2 (6)	1.3 (6)	
<sup>43</sup> K	(p, n)	1.5 (4)	2.4 (4)	(14)		(p, γ)	1.7 (3)	2.7 (3)	
	(p, γ)	5.1 (2)	8.2 (2)		<sup>49</sup> Ti	(n, γ)	1.5 (6)	1.5 (6)	
<sup>46</sup> K	(γ, n)	6.0 (-1)	1.4 (1)	(8)		(p, n) *	2.1 (3)	4.1 (3)	
						(p, γ) *	6.3 (2)	9.3 (2)	



TABLE 1—Continued

Target	Reaction	$N_A < \sigma v <$		Ref <sup>(1)</sup>	Target	Reaction	$N_A < \sigma v <$		Ref <sup>(1)</sup>
		$T_9 = 2.00$	$T_9 = 2.15$				$T_9 = 2.00$	$T_9 = 2.15$	
<sup>50</sup> Ti	(n, $\gamma$ )	3.0 (5)	3.3 (5)		<sup>71, 73</sup> Cu	(p, n) *	5.0 (2)	1.0 (3)	(2)
	(p, $\gamma$ )	1.8 (4)	2.9 (4)			( $\gamma$ , n) *	2.0 (0)	2.3 (1)	(8)
<sup>51</sup> Ti	(p, n)	2.7 (3)	4.6 (3)		<sup>63</sup> Fe	( $\gamma$ , n) *!	3.9 (2)	3.1 (3)	(8)
<sup>47</sup> V	(n, $\gamma$ )	1.2 (5)	1.8 (5)		<sup>65</sup> Fe	( $\gamma$ , n) *!	8.7 (3)	4.6 (5)	(8)
	(n, p)	5.9 (8)	5.7 (8)			( $\gamma$ , n)	4.9 (0)	6.3 (1)	(8)
<sup>48</sup> V	(n, $\gamma$ )	1.3 (7)	1.3 (7)		<sup>66</sup> Co	( $\gamma$ , n) *	1.7 (3)	1.4 (4)	(8)
	(n, p)	2.1 (7)	2.3 (7)		<sup>68</sup> Co	( $\gamma$ , n) *	4.5 (4)	2.9 (5)	(8)
	(p, $\gamma$ )	1.3 (3)	2.1 (3)			( $\gamma$ , n) *	3.0 (1)	2.8 (2)	(8)
<sup>49</sup> V	(n, $\gamma$ )	8.3 (6)	8.4 (6)		<sup>67</sup> Ni	( $\gamma$ , n) *	6.0 (2)	4.4 (3)	(8)
	(n, p)	6.9 (6)	7.6 (6)		<sup>69</sup> Ni	( $\gamma$ , n) *!	1.9 (4)	1.1 (5)	(8)
	(p, $\gamma$ )	1.6 (3)	2.6 (3)			( $\gamma$ , n) *	3.1 (1)	3.6 (2)	(8)
<sup>50</sup> V	(n, $\gamma$ )	1.6 (6)	2.5 (6)		<sup>71</sup> Ni	( $\gamma$ , n) *	1.3 (3)	1.1 (4)	(8)
	(p, n)	9.9 (3)	1.8 (4)		<sup>70</sup> Cu	( $\gamma$ , n) *	6.1 (2)	5.6 (3)	(8)
	(p, $\gamma$ )	1.2 (5)	1.9 (5)			( $\gamma$ , n) *	3.9 (1)	3.5 (2)	(8)
	(n, p) *	3.9 (7)	4.1 (7)		<sup>77</sup> Zn	( $\gamma$ , n) *	1.0 (3)	7.4 (3)	(8)
Fe-Zn	(n, $\gamma$ )	-	-	(15)					
<sup>62, 64</sup> Fe	(p, n) *!	1.1 (3)	2.0 (3)	(2)					
<sup>65, 67</sup> Co	(p, n) *	1.1 (3)	2.0 (3)	(2)					
<sup>68, 70</sup> Ni	(p, n) *!	5.0 (2)	1.0 (3)	(2)					

## NOTES TO TABLE 1

\* Important reaction rate.

\*! Very important reaction rate.

(1) Rates for which no reference number is given are due to a private communication from James Truran (1971), who has made an extensive study, largely unpublished, of thermonuclear reaction rates.

(2) Our estimate.

(3) Chosen equal to  $^{33}\text{S}(n, \gamma)^{34}\text{S}$ .(4) Our estimate. Same value is chosen for (n,  $\gamma$ ) rate on  $^{39, 41, 43, 45}\text{Cl}$ .(5) Fowler *et al.* (1971).(6) Our estimate. Same value is chosen for (n,  $\gamma$ ) rate on  $^{38, 40, 42, 44, 46}\text{Cl}$ .(7) Truran (1971). Same value is chosen for (p, n) on  $^{39, 40, 41, 42, 43, 44, 45, 46}\text{Cl}$ . Reverse rates depend on semiempirical masses of Garvey *et al.* (1969).(8) Rates based on semiempirical ( $\gamma$ , n) thresholds of Garvey *et al.* (1969).(9) Our estimate. Same value is chosen for (n,  $\gamma$ ) rates on  $^{41, 43, 45, 47}\text{Ar}$ .(10) Our estimate. Same value is chosen for (n,  $\gamma$ ) rates on  $^{42, 44, 46}\text{Ar}$ .(11) Truran (1971). Same value is chosen for (p, n) rates on  $^{42, 43, 44, 45, 46, 47}\text{Ar}$ . Reverse rates depend on semiempirical masses of Garvey *et al.* (1969).(12) Our estimate. Same value is chosen for (n,  $\gamma$ ) rates on  $^{42, 44, 46, 48}\text{K}$ .(13) Truran (1971). Same value is chosen for (p, n) rates on  $^{44, 46, 48, 50}\text{K}$ . Reverse rates depend on semiempirical masses of Garvey *et al.* (1969).(14) Truran (1971). Same value is chosen for (p, n) rates on  $^{45, 47, 49}\text{K}$ . Reverse rate of  $^{49}\text{K}(p, n)^{49}\text{Ca}$  depends on semiempirical masses of Garvey *et al.* (1969).

(15) These rates unimportant. See text.

tions at the three characteristic peak temperatures  $T_9 = 2.00$ , 2.05, and 2.15. These three temperatures provide a sufficiently wide variation of free-particle densities that we are able to ascertain the characteristics of the seed nucleosynthesis. Because we regard the hydrodynamic timescale as being related to the density, it will have the same value—i.e.,  $\tau_p = 1.4$  seconds—for each of the three calculations reported here. We will not defend this simplification except by noting that the nature of the burning depends much more strongly on temperature than on timescale. Nonetheless we acknowledge that the calculations we report here are only a sketchy survey of carbon burning.

### b) Source of Free Particles

Figure 1 shows the free-proton and free-neutron mass fractions as a function of time for three temperatures. At  $t = 0.1$  s the density has decreased by only 7 percent and the temperature by only 2 percent. A general feature of the profiles is that the neutrons dominate for the first  $10^{-1}$  s, which for convenience we will call the "neutron-dominated phase," after which the protons dominate for the final second, which we will call the "proton-dominated phase." It is when these two phases overlap that the most complicated alteration of the seed nuclei take place. All of the features of figure 1 are determined by the basic carbon-burning reactions.

Approximately 2 percent by mass of the shell is assumed to be initially in the form of an  $^{18}\text{O}$  residue from the previous CNO cycle and helium burning. The  $^{18}\text{O}$  provides the major free-neutron source by  $(\alpha, n)$  reactions. If the  $^{18}\text{O}$  were transmuted on to  $^{22}\text{Ne}$  during helium burning, the nucleon densities would differ somewhat from those we will use, but the basic systematics will be similar. The neutron densities encountered during explosive carbon burning (typically  $n_n = 10^{18}$ – $10^{21}$   $\text{cm}^{-3}$ ) are lower than the neutron densities usually required for  $r$ -process calculations ( $n_n \simeq 10^{24}$   $\text{cm}^{-3}$ ) but much higher than neutron densities assumed for the  $s$ -process ( $n_n \approx 10^{10}$   $\text{cm}^{-3}$ ). We therefore expect the capture process to be somewhat intermediate to the conventional  $s$ - and  $r$ -process pictures, and indeed that turns out to be the case. The temperatures are high enough that the photodisintegration rates of some nuclei of low neutron separation energy become important and the neutron-capture flow is stopped by  $(\gamma, n)$  reactions. Unlike the traditional  $r$ -process, however, the increase in  $Z$  is accomplished by  $(p, n)$  reactions rather than by  $\beta$ -decays.

To the extent that the capture is like the  $r$ -process, the resulting abundances depend more upon neutron separation energies (that are unmeasured) than on the rates of  $(n, \gamma)$  reactions. Proton-induced reactions, though slower than neutron-induced reactions, perform the role of increasing the nuclear charge and in modifying abundances when the neutron source is nearly exhausted.

At  $T_9 = 2.15$ , the source of free protons is the proton channel of carbon burning and, in the later stages of the burning,  $(\alpha, p)$  reactions primarily on  $^{23}\text{Na}$ . The primary importance of this proton density is due to the  $(p, n)$  reactions it causes on neutron-rich isotopes. We have not examined the extent to which the proton density is altered by

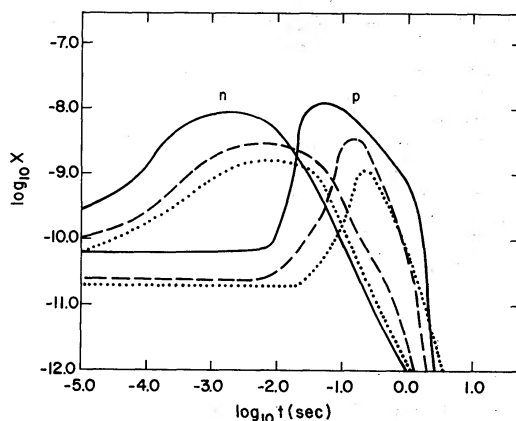


FIG. 1.—The mass fractions of free protons and neutrons are shown as a function of time during explosive carbon burning from initial density  $\rho_0 = 10^6$   $\text{g cm}^{-3}$ . Solid curve, densities at  $T_9 = 2.15$ ; dashed curve, those at  $T_9 = 2.05$ ; dotted curve, those at  $T_9 = 2.00$ . The most complicated nuclear flows at  $T_9 = 2.15$  take place between  $10^{-2}$  and  $10^{-1}$  s when both the proton and neutron fluxes are relatively high. Notice that the integrated proton flux is much larger at  $T_9 = 2.15$  than at  $T_9 = 2.05$  or  $2.00$ , in contrast to the integrated neutron flux.

changes of the initial composition or hydrodynamic timescale because investigation of those questions does not seem to be necessary at the present level of accuracy.

c) Numerical Results

Table 2 lists the overabundances, defined as the ratio of the yield by mass  $X$  of each nuclear species produced by our three trial calculations to the mass fraction  $X_{\odot}$  of that species in solar material. For example, the fact that  $X/X_{\odot} = 186$  for  $^{24}\text{Mg}$  in the  $T_9 = 2.15$  explosion means that the  $^{24}\text{Mg}$  concentration is 186 times greater after the explosion than it was before it; furthermore, it allows (but certainly does not demand) the simple interpretation that all of the natural  $^{24}\text{Mg}$  abundance was synthesized in this way when  $1/186$  of all galactic matter passed through these carbon explosions. That  $X/X_{\odot} = 180$  for  $^{36}\text{S}$  implies that if that picture were correct, the natural  $^{36}\text{S}$  abundance would have been synthesized from  $^{32}\text{S}$  and  $^{36}\text{Ar}$  seed nuclei in the same events. That  $X/X_{\odot} = 1490$  for  $^{71}\text{Ga}$  would, on the other hand, imply that  $^{71}\text{Ga}$  would be overproduced by the factor  $1490/186 = 8$  in the same events if all of the nuclear details were accurate. Similarly only 21 percent of the  $^{43}\text{Ca}$  would have been synthesized, etc. Nonetheless, the results are astonishing in that all species listed in table 2 are coproduced to within a factor of 8 by that simple hypothesis, and  $^{36}\text{S}$ ,  $^{40}\text{Ar}$ ,  $^{40}\text{K}$ ,  $^{48}\text{Ca}$ ,  $^{45}\text{Sc}$ ,  $^{47}\text{Ti}$ ,  $^{49}\text{Ti}$ ,  $^{50}\text{Ti}$ ,  $^{50}\text{V}$ ,  $^{62}\text{Ni}$ ,  $^{64}\text{Ni}$ ,  $^{65}\text{Cu}$ ,  $^{68}\text{Zn}$ ,  $^{69}\text{Ga}$ ,  $^{75}\text{As}$ , and  $^{76}\text{Ge}$  are coproduced to within a factor 3.

The results are quite temperature sensitive. For example, at  $T_9 = 2.00$  the  $^{71}\text{Ga}$  now has negligible yield. The largest overproduction now belongs to  $^{46}\text{Ca}$ , which is 67 times more overabundant than  $^{23}\text{Na}$ , the most overabundant product of the carbon burning. These three columns of table 2 were calculated with the same cross-sections and  $Q$ -values, so we may infer that even if the nuclear physics were exactly known, the identity of the

TABLE 2  
OVERABUNDANCES PRODUCED

PRODUCT	PRIMARY SEED	$X/X_{\odot}$		
		$T_9 = 2.15$	$T_9 = 2.05$	$T_9 = 2.00$
$^{20}\text{Ne}$ .....	C-burn	134	117	77
$^{23}\text{Na}$ .....	C-burn	56	78	102
$^{24}\text{Mg}$ .....	C-burn	186	82	44
$^{36}\text{S}$ .....	$^{32}\text{S}$ , $^{36}\text{Ar}$	180	1000	1100
$^{40}\text{Ar}$ .....	$^{36}\text{Ar}$ , $^{32}\text{S}$	300	220	110
$^{40}\text{K}$ .....	$^{36}\text{Ar}$ , $^{32}\text{S}$	290	28	1.6
$^{43}\text{Ca}$ .....	$^{36}\text{Ar}$	39	46	50
$^{46}\text{Ca}$ .....	$^{36}\text{Ar}$ , $^{40}\text{Ca}$	730	3200	6700
$^{48}\text{Ca}$ .....	$^{40}\text{Ca}$	110	170	140
$^{45}\text{Sc}$ .....	$^{36}\text{Ar}$	95	350	570
$^{47}\text{Ti}$ .....	$^{40}\text{Ca}$ , $^{36}\text{Ar}$	86	230	130
$^{49}\text{Ti}$ .....	$^{40}\text{Ca}$	290	45	23
$^{50}\text{Ti}$ .....	$^{40}\text{Ca}$	68	58	58
$^{50}\text{V}$ .....	$^{40}\text{Ca}$	72	4.2	Small
$^{62}\text{Ni}$ .....	$^{56}\text{Fe}$	190	300	320
$^{64}\text{Ni}$ .....	$^{56}\text{Fe}$	225	520	560
$^{65}\text{Cu}$ .....	$\text{Fe}(p, n)$	930	205	57
$^{67}\text{Zn}$ .....	$\text{Fe}(p, n)$	690	510	170
$^{68}\text{Zn}$ .....	$^{58, 60}\text{Ni}$	450	140	130
$^{70}\text{Zn}$ .....	$^{58, 60}\text{Ni}$	1060	800	750
$^{69}\text{Ga}$ .....	$\text{Ni}(p, n)$	170	Small	Small
$^{71}\text{Ga}$ .....	$\text{Ni}(p, n)$	1490	110	44
$^{73}\text{Ge}$ .....	$\text{Ni}(p, n)$	770	84	34
$^{75}\text{As}$ .....	$\text{Ni}(p, n)$	127	68	34
$^{76}\text{Ge}$ .....	Zn	200	110	110

most overabundant products would shift with changing explosive conditions. The overabundances of many of these species, moreover, depend critically on unknown nuclear quantities, as we shall emphasize in § IV.

This order-of-magnitude success is nearly complete. Table 2 contains every rare neutron-rich nucleus between  $36 \leq A \leq 76$  except  $^{54}\text{Cr}$ ,  $^{58}\text{Fe}$ , and  $^{61}\text{Ni}$ . Because these systems of reactions necessarily occur in explosive carbon burning, we tentatively draw the following conclusion: a significant fraction of the natural abundance of all the nuclei listed in table 2 was synthesized in explosive carbon burning if  $^{23}\text{Na}$  and  $^{24}\text{Mg}$  were, but  $^{54}\text{Cr}$ ,  $^{58}\text{Fe}$ , and  $^{61}\text{Ni}$  do not seem to have been so synthesized. The possible *s*-process origins of these last three nuclei have recently been analyzed by Peters, Fowler, and Clayton (1972); a significant amount of  $^{61,62}\text{Ni}$  is produced in the dynamic *e*-process discussed by Arnett *et al.* (1971).

#### IV. NUCLEAR DETAILS

This discussion will center on the key reactions and nuclear facts that determine the yields of the important products listed in table 2. In so doing we will concentrate on our calculations at  $T_9 = 2.15$  because the most complex nucleosynthesis happens in this case. Because of the higher proton density and temperature, the (*p*, *n*) reactions play a much more important role than at the two lower temperatures.

A significant understanding of this problem is aided by knowledge of the seed nucleus responsible for the rare products. We made a thorough investigation of this at  $T_9 = 2.15$  by performing separate calculations with only a single seed nucleus (one of the group  $^{32}\text{S}$ ,  $^{34}\text{S}$ ,  $^{36}\text{Ar}$ ,  $^{38}\text{Ar}$ , and  $^{40}\text{Ca}$  in turn). Because the differential equations are linear in the abundance, the yield from a weighted sum of seed nuclei is equal to the weighted yields from the single seed nuclei. Table 3 lists the contributions from the five most abundant seed nuclei between silicon and chromium to the final yields of rare nuclei in the same mass range. One immediately sees that the sum of the yields from these five seeds, shown in the last column, completely dominates the total yield from the complete set of seed nuclei, which is shown in the first column. It is also clear that the origins of the several species are rather widely distributed among seed nuclei. We now turn our attention to the specific nuclear reactions by which this comes about.

##### a) $^{36}\text{S}$

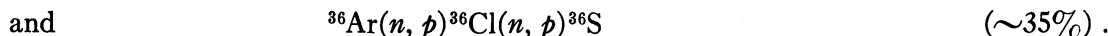
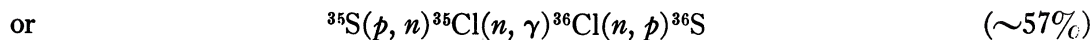
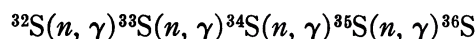
One of the most interesting features of our calculations is the production of  $^{36}\text{S}$ . As we can see from table 3,  $^{36}\text{S}$  has  $^{32}\text{S}$ ,  $^{34}\text{S}$ , and  $^{36}\text{Ar}$  as its primary sources and is produced

TABLE 3  
PARTIAL CONTRIBUTIONS FROM PRINCIPAL SEED AT  $T_9 = 2.15$

PRODUCT NUCLEUS	TOTAL SEED YIELD $X$	PARTIAL MASS FRACTION $X_i$ DUE TO SEED $i$					FIVE-SEED YIELD $\Sigma X_i$
		$i = ^{32}\text{S}$	$^{34}\text{S}$	$^{36}\text{Ar}$	$^{38}\text{Ar}$	$^{40}\text{Ca}$	
$^{36}\text{S}$ .....	1.37(-5)	0.62(-5)	0.17(-5)	0.48(-5)	0.01(-5)	0.03(-5)	1.31(-5)
$^{40}\text{Ar}$ .....	3.42(-6)	1.15(-6)	0.44(-6)	1.64(-6)	0.04(-6)	0.11(-6)	3.40(-6)
$^{40}\text{K}$ .....	1.44(-6)	0.54(-6)	0.18(-6)	0.62(-6)	0.02(-6)	0.04(-6)	1.40(-6)
$^{43}\text{Ca}$ .....	5.12(-6)	0.55(-6)	0.26(-6)	3.85(-6)	0.07(-6)	0.22(-6)	4.95(-6)
$^{46}\text{Ca}$ .....	2.31(-6)	0.08(-6)	0.04(-6)	1.31(-6)	0.25(-6)	0.60(-6)	2.28(-6)
$^{48}\text{Ca}$ .....	1.97(-5)	0.01(-5)	0.00(-5)	0.33(-5)	0.30(-5)	1.24(-5)	1.88(-5)
$^{45}\text{Sc}$ .....	4.02(-6)	0.22(-6)	0.12(-6)	2.57(-6)	0.30(-6)	0.75(-6)	3.96(-6)
$^{47}\text{Ti}$ .....	1.94(-5)	0.02(-5)	0.01(-5)	0.66(-5)	0.33(-5)	0.88(-5)	1.90(-5)
$^{49}\text{Ti}$ .....	5.07(-5)	0.02(-5)	0.01(-5)	0.81(-5)	0.75(-5)	3.19(-5)	4.78(-5)
$^{50}\text{Ti}$ .....	1.19(-5)	0.00(-5)	0.00(-5)	0.09(-5)	0.10(-5)	0.89(-5)	1.08(-5)
$^{50}\text{V}$ .....	2.26(-7)	0.01(-7)	0.01(-7)	0.40(-7)	0.33(-7)	1.38(-7)	2.13(-7)



by the following reaction sequences:



Needless to say, the rates of these reactions play an important role in determining the final yield of  $^{36}\text{S}$ . In figure 2 we show selected currents (which govern the yield of  $^{36}\text{S}$ ) as a function of time, defined as  $J_{n,i;k,l} = Y_n V_i \rho N_A \langle \sigma v \rangle_{i,k,l}$ . Physically  $J_{n,i;k,l}$  is the contribution of the forward rate of the reaction  $n(i, k)l$  to the time rate of change, for nuclear species  $n$ , of its abundance  $Y_n$  ( $Y_n \equiv X_n/A_n$ ). We see that  $^{36}\text{Ar}$  quickly flows toward  $^{36}\text{S}$  as the  $^{36}\text{Cl}(n, p)^{36}\text{S}$  reaction current equilibrates early with  $^{36}\text{Ar}(n, p)^{36}\text{Cl}$ ; however, the latter current has a late surge due to the arrival of current from  $^{32}\text{S}$  seed via  $^{35}\text{S}(p, n)^{35}\text{Cl}(n, \gamma)^{36}\text{Cl}$ . The contribution from  $^{32}\text{S}$  seed is attenuated by the large rate of the exothermic reaction  $^{33}\text{S}(n, \alpha)^{30}\text{Si}$ . Truran (1971) calculates the ratio of decay widths of the compound nuclear states of  $^{34}\text{S}$  as  $\Gamma_\alpha/\Gamma_\gamma \approx 22$ . This branching ratio is important because  $^{36}\text{S}$  is easy to produce. It shows especially large overabundances at  $T_9 = 2.05$  and  $2.00$  in table 2, and a reduction in the ratio of decay widths would cause increased overabundances. Conversely, if the branching ratio was large enough to prevent the contribution of  $^{32}\text{S}$  seed to  $^{36}\text{S}$ , table 3 shows that at  $T_9 = 2.15$  the yield of  $^{36}\text{S}$  would be reduced by a factor 2. Thus the rate of  $^{33}\text{S}(n, \alpha)^{30}\text{Si}$  has an important bearing on the yield of  $^{36}\text{S}$ . The values of the radiative neutron-capture cross-sections for sulfur also enter critically in the final yield of  $^{36}\text{S}$ . We have taken the rate of  $^{34}\text{S}(n, \gamma)^{35}\text{S}$  to be the smallest neutron-capture rate in the sulfur chain, and as a result almost 10 times as much mass remains in  $^{34}\text{S}$  as remains in  $^{36}\text{S}$  at the end of the calculation. An increase in this rate could increase the final yield of  $^{36}\text{S}$  by a substantial amount. The  $^{34}\text{S}$  is due to  $^{32}\text{S}$  seed and to the  $^{37}\text{Cl}(p, \alpha)^{34}\text{S}$  reaction.

As we can see from figure 2, the  $^{36}\text{S}$  is built to a high abundance during the neutron-dominated phase and then is destroyed by  $^{36}\text{S}(p, \gamma)^{37}\text{Cl}$  in the proton-dominated phase. At  $T_9 = 2.15$  the abundance of  $^{36}\text{S}$  is reduced by an order of magnitude from its peak value by the  $(p, \gamma)$  reactions, and it is the relative weakness of the proton flux at  $T_9 = 2.00$  and  $2.05$  that results in the larger overabundance of  $^{36}\text{S}$  at those temperatures. In fact, we have found that the final yield of  $^{36}\text{S}$  varies inversely with the rate of  $^{36}\text{S}(p, \gamma)^{37}\text{Cl}$ . For example, at  $T_9 = 2.05$ , we increased Truran's value for this rate by a factor 5

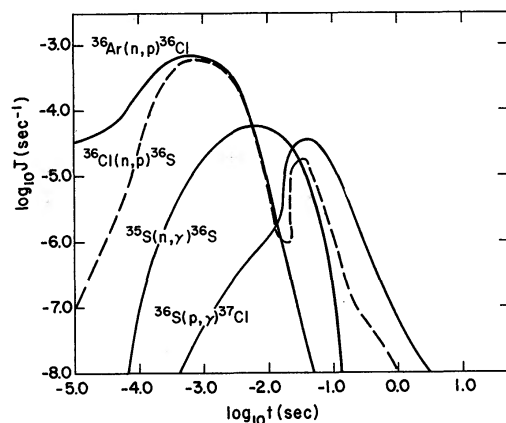


FIG. 2.—Some important reaction currents  $J$  involved in the synthesis of  $^{36}\text{S}$  are shown as a function of time during the burning at  $T_9 = 2.15$ . The source of  $^{36}\text{Cl}(n, p)^{36}\text{S}$  after the  $^{36}\text{Ar}$  is exhausted is the reaction sequence  $^{35}\text{S}(p, n)^{35}\text{Cl}(n, \gamma)^{36}\text{Cl}$ . At this temperature the proton flux is sufficient to reduce the yield of  $^{36}\text{S}$  by almost an order of magnitude.

and found a decrease in the yield of  $^{36}\text{S}$  by about the same factor, making its overabundance comparable to those of the primary products of carbon burning. However, in this experiment we have exchanged one embarrassing result for another—there results a comparable overabundance of  $^{37}\text{Cl}$ . There exists ample evidence that  $^{37}\text{Cl}$  owes its thermonuclear origin primarily to explosive-oxygen-burning phases; thus to produce it here could cause an overproduction. At  $T_9 = 2.15$ , on the other hand, the  $^{37}\text{Cl}$  is not produced because the proton flux is sufficient to destroy the  $^{37}\text{Cl}$ , mostly by  $(p, \alpha)$  reactions back to  $^{34}\text{S}$ . We see here the tendency to establish a loop involving  $^{34}\text{S}$ ,  $^{36}\text{S}$ , and  $^{37}\text{Cl}$ , and the value of each cross-section in this loop is important, as are the  $(n, \gamma)$  and  $(p, \gamma)$  reactions on  $^{37}\text{Cl}$  that cause leaks from the loop.

We conclude that the rates of  $^{36}\text{S}(p, \gamma)^{37}\text{Cl}$ ,  $^{37}\text{Cl}(p, \alpha)^{34}\text{S}$ ,  $^{34}\text{S}(n, \gamma)^{35}\text{S}$ , and the branching ratio in the compound nuclear states of  $^{34}\text{S}$ ,  $^{37}\text{Ar}$ , and  $^{38}\text{Ar}$  formed by  $^{33}\text{S} + n$ ,  $^{36}\text{Ar} + n$ , and  $^{37}\text{Cl} + p$ , respectively, are vital in determining the yield of  $^{36}\text{S}$  and, by our basic assumption, placing constraints on the conditions that produce the Mg isotopes in nature.

#### b) $^{40}\text{Ar}$

We should first mention that the solar-system abundance of  $^{40}\text{Ar}$  is very uncertain. Cameron (1968) estimated its abundance by assuming that  $^{36}\text{S}$ ,  $^{40}\text{Ar}$ , and  $^{46}\text{Ca}$  are synthesized by the same thermonuclear processes and should have roughly the same abundance. Since the abundance of  $^{40}\text{Ar}$  is not experimentally determined, we should not place heavy emphasis on the agreement of our calculated value with Cameron's value. By the same token, an experimental determination of solar  $^{40}\text{Ar}$  is badly needed.

As seen from table 3 the major sources of  $^{40}\text{Ar}$  (made as itself) are  $^{36}\text{Ar}$  (~48 percent),  $^{32}\text{S}$  (~33 percent), and  $^{34}\text{S}$  (~13 percent). The initial neutron flow in the argon isotopes bypasses  $^{40}\text{Ar}$  since the flow is not halted until it encounters the low neutron separation energies of  $^{45}\text{Ar}$  and  $^{47}\text{Ar}$ . During the proton-dominated phase the  $^{40}\text{Ar}$  is made from the destruction of  $^{36}\text{S}$  by the following reaction sequences:  $^{36}\text{S}(p, \gamma)^{37}\text{Cl}(n, \gamma)^{38}\text{Cl}(n, \gamma)^{39}\text{Cl}(p, n)^{39}\text{Ar}(n, \gamma)^{40}\text{Ar}$ , and  $^{36}\text{S}(p, \gamma)^{37}\text{Cl}(p, \gamma)^{38}\text{Ar}(n, \gamma)^{39}\text{Ar}(n, \gamma)^{40}\text{Ar}$ . The  $^{40}\text{Ar}$  is partially destroyed in the expansion by  $^{40}\text{Ar}(p, \gamma)^{41}\text{K}$ . The rates of  $^{36}\text{S}(p, \gamma)^{37}\text{Cl}$ ,  $^{39}\text{Ar}(n, \gamma)^{40}\text{Ar}$ , and  $^{40}\text{Ar}(p, \gamma)^{41}\text{K}$  enter critically in determining the final yields.

#### c) $^{40}\text{K}$

The radioactive species  $^{40}\text{K}$  has a half-life  $\tau_{1/2} = 1.26 \times 10^9$  years, and its yield is not accounted for in ordinary explosive oxygen or silicon burning. In our calculation at  $T_9 = 2.15$  its overabundance is 1.6 times greater than the overabundance of the primary product  $^{24}\text{Mg}$ . At the two lower temperatures its overabundance seems insignificant. These overabundances, moreover, are with respect to the abundance  $^{40}\text{K} = 4.3$  per  $10^6$  silicon atoms in the solar nebula. The total production by continuous nucleosynthesis must exceed this value by a factor of 5–10 to account for its decay between nucleosynthesis and formation of the solar nebula. Thus we regard our present calculations as encouraging, but not quite adequate to explain the natural abundance of  $^{40}\text{K}$ .

As mentioned previously, the  $^{40}\text{K}$  is produced in the proton phase at  $T_9 = 2.15$  by the reaction sequence  $^{36}\text{S}(p, \gamma)^{37}\text{Cl}(p, \gamma)^{38}\text{Ar}(p, \gamma)^{39}\text{K}(n, \gamma)^{40}\text{K}$ . The  $(p, \gamma)$  reactions enter critically, of course, as does the rate of  $^{39}\text{K}(n, \gamma)^{40}\text{K}$ , which we have inferred from Allen *et al.* (1971).

Calculation of the  $^{40}\text{K}$  abundance remains an exciting possibility. Once a viable theory for the formation of  $^{40}\text{K}$  is determined, we will have another constraint for calculations of nuclear cosmochronology. Perhaps it has more than one source. Peters *et al.* (1972) showed that it may have significant contributions from weak s-process irradiations.

#### d) $^{43}\text{Ca}$ , $^{44}\text{Ca}$ , and $^{46}\text{Ca}$

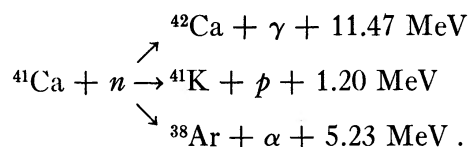
At  $T_9 = 2.15$ , the relative production of  $^{43}\text{Ca}$  is a factor of 5 below that of  $^{24}\text{Mg}$ ,  $^{44}\text{Ca}$  is a factor 100 below it, and  $^{46}\text{Ca}$  is overproduced by a factor 4. The  $(n, \gamma)$  chain in

calcium flows through these nuclei without substantial residual. They are produced instead in the proton phase when the neutrons are almost exhausted. The  $^{43}\text{Ca}$  is produced as  $^{43}\text{Ca}$  ( $\sim 63$  percent),  $^{43}\text{K}$  ( $\sim 18$  percent), and  $^{43}\text{Cl}$  ( $\sim 18$  percent), with  $^{36}\text{Ar}$  ( $\sim 75$  percent) as its primary source through the reaction sequence  $^{36}\text{Ar}(n, p)^{36}\text{Cl}(n, p)^{36}\text{S}(p, \gamma)^{37}\text{Cl}(p, \gamma)^{38}\text{Ar}(n, \gamma)^{39}\text{Ar}(n, \gamma)^{40}\text{Ar}(n, \gamma)^{41}\text{Ar}(n, \gamma)^{42}\text{Ar}(p, n)^{42}\text{K}(n, \gamma)^{43}\text{K}(p, n)^{43}\text{Ca}$ . The rates of the unmeasured  $(p, n)$  reactions on  $^{42}\text{Ar}$  and  $^{43}\text{K}$ , as well as the neutron separation energy of  $^{43}\text{Ar}$ , are critical in determining the final yields. An interesting feature of this calculation is the way the  $(p, \gamma)$ ,  $(p, n)$ , and  $(n, \gamma)$  reactions interplay in rearranging the  $^{36}\text{S}$  into higher-mass nuclei. The  $^{43}\text{Cl}$  contribution to  $^{43}\text{Ca}$  results from the sequence  $^{36}\text{S}(p, \gamma)^{37}\text{Cl}(n, \gamma) \dots ^{42}\text{Cl}(n, \gamma)^{43}\text{Cl}$ , where the low neutron separation energy of  $^{44}\text{Cl}$  (unmeasured) stops the neutron flow by  $(\gamma, n)$  reactions.

At  $T_9 = 2.05$ , if we increase the rate of  $^{36}\text{S}(p, \gamma)^{37}\text{Cl}$  to eliminate the  $^{36}\text{S}$  overproduction as described earlier, the yield of  $^{43}\text{Ca}$  is close to its solar-system value relative to  $^{24}\text{Mg}$ . Under this circumstance, however, the  $^{43}\text{Ca}$  is produced by the sequence  $^{36}\text{Ar}(n, \gamma)^{37}\text{Ar}(n, p)^{37}\text{Cl}(n, \gamma) \dots ^{42}\text{Cl}(n, \gamma)^{43}\text{Cl}$ , where again the low  $^{44}\text{Cl}$  neutron separation energy halts the flow. This  $Q$ -value, along with the rate of  $^{37}\text{Ar}(n, p)^{37}\text{Cl}$  enter critically into the result.

The  $^{44}\text{Ca}$  is produced as itself in a way similar to  $^{43}\text{Ca}$ . None of the calculations come close to producing a large  $^{44}\text{Ca}$  overabundance, however, so we do not think that this process is an important contributor to the  $^{44}\text{Ca}$  abundance. Indeed, we did not in advance regard  $^{44}\text{Ca}$  as a "rare neutron-rich nucleus"; surely it is synthesized in an  $\alpha$ -particle process as  $^{44}\text{Ti}$ . For the process described here there is simply an insufficient amount of available seed. Essentially all of the  $^{32}\text{S}$  would have to be converted into  $^{44}\text{Ca}$  to account for its solar-system abundance. We will not consider  $^{44}\text{Ca}$  further, and it is not entered in table 2.

The  $^{46}\text{Ca}$  (created as itself) has the primary sources  $^{36}\text{Ar}$  ( $\sim 57$  percent) and  $^{40}\text{Ca}$  ( $\sim 26$  percent) through the sequences  $^{36}\text{Ar}(n, \gamma)^{37}\text{Ar}(n, p)^{37}\text{Cl}(n, \gamma) \dots ^{45}\text{Cl}(p, n)^{45}\text{Ar}(\gamma, n)^{44}\text{Ar}(p, n)^{44}\text{K}(n, \gamma)^{45}\text{K}(p, n)^{45}\text{Ca}(n, \gamma)^{46}\text{Ca}$ , and also  $^{40}\text{Ca}(n, \gamma)^{41}\text{Ca}(n, \alpha)^{38}\text{Ar}(n, \gamma) \dots ^{44}\text{Ar}(p, n)^{44}\text{K}(n, \gamma)^{45}\text{K}(p, n)^{45}\text{Ca}(n, \gamma)^{46}\text{Ca}$ . These snakelike chains have a kind of fascination, and the reader will easily spot nuclear question marks. The branching ratios of the three decay modes of  $^{42}\text{Ca}$  are becoming very important:



The Coulomb barrier for an  $\alpha$ -particle in an  $^{38}\text{Ar}$  nucleus is only  $E_{\text{Coul}} = 7.85$  MeV, so the  $\alpha$ -channel is not inhibited much. We have taken the ratio of the branching to be  $\Gamma_\alpha : \Gamma_p : \Gamma_\gamma = 8.78 : 2.39 : 4.22$ . The amount of  $^{40}\text{Ca}$  seed that can be converted into  $^{43}\text{Ca}$  and  $^{46}\text{Ca}$  is dependent upon the  $\alpha$ -particle branch. It is important to measure these three branching ratios in order to calculate the yields of  $^{46}\text{Ca}$  under explosive conditions, in addition to the rates for  $^{37}\text{Ar}(n, p)^{37}\text{Cl}$ ,  $^{37}\text{Cl}(n, \gamma)^{38}\text{Cl}$ ,  $^{45}\text{Cl}(p, n)^{45}\text{Ar}(p, n)^{45}\text{K}(p, n)^{45}\text{Ca}$ ,  $^{45}\text{Ca}(n, \gamma)^{46}\text{Ca}$ , and  $^{46}\text{Ca}(n, \gamma)^{47}\text{Ca}$ . Perhaps with improved cross-section information the relative overproduction of  $^{46}\text{Ca}$  may disappear.

The  $^{46}\text{Ca}$  yield also depends on unknown neutron separation energies in neutron-rich matter—especially that of  $^{45}\text{Ar}$ . We used  $Q = 5.21$  MeV for  $^{44}\text{Ar}(n, \gamma)^{45}\text{Ar}$  from Garvey *et al.* (1969), but quite acceptable uncertainties in this number change greatly the fraction of the argon  $(n, \gamma)$  flow that can reach  $^{46}\text{Ar}$ , and at lower temperatures a significant fraction of the  $^{46}\text{Ca}$  is made in this way. To check this conclusion numerically we repeated the calculations with the  $Q$ -value reduced by 400 keV. The much smaller concentration of  $^{45}\text{Ar}$ , in equilibrium with  $^{44}\text{Ar}$  and neutrons, allowed only a much reduced flow into  $^{46}\text{Ar}$ . This had no effect on the yield at  $T_9 = 2.15$  which, as we just explained, is

controlled by  $(p, n)$  flows; but it reduced the  $^{46}\text{Ca}$  overabundance at  $T_9 = 2.00$  by a factor of 5. We are thus not too discouraged by the very large overabundances of  $^{46}\text{Ca}$  listed at  $T_9 = 2.00$  in table 2, as it could easily be reduced by a factor of 50 with moderate changes in nuclear cross-sections and  $Q$ -values. Nonetheless it is probably the most serious systematic obstacle to synthesis near  $T_9 = 2.0$ , so it bears watching. As usual, only better nuclear facts can provide the answer. The  $^{48}\text{Ca}$  is produced as itself from the sources  $^{40}\text{Ca}$ ,  $^{36}\text{Ar}$ , and  $^{38}\text{Ar}$ . This is the first product for which  $^{40}\text{Ca}$  dominates  $^{36}\text{Ar}$  and  $^{38}\text{Ar}$  as a source and is the result of the impediment of the neutron flow in the calcium isotopes by a  $(\gamma, n)$  reaction on  $^{49}\text{Ca}$ . Nonetheless, measurements of  $^{48}\text{Ca}(n, \gamma)^{49}\text{Ca}$  are needed. The  $^{48}\text{Ca}$  abundance is also reduced by a factor 2 by  $(p, \gamma)$  reactions as the neutrons are exhausted. Measurements of that radiative capture are needed. The  $^{36}\text{Ar}$  and  $^{38}\text{Ar}$  is converted to  $^{48}\text{Ca}$  via long sequences of  $(n, \gamma)$  and  $(p, n)$  chains (see  $^{46}\text{Ca}$  and  $^{47}\text{Ti}$ ). Because the yield from  $^{40}\text{Ca}$  seed is primarily due to  $(n, \gamma)$  reactions in calcium, it is proportional to the  $(n, \gamma)$  branch of  $^{41}\text{Ca} + n$ , again emphasizing the importance of laboratory measurements of  $^{41}\text{Ca} + n$  (see fig. 3).

e)  $^{45}\text{Sc}$

The  $^{45}\text{Sc}$  is produced as  $^{45}\text{Sc}$  ( $\sim 45$  percent),  $^{45}\text{Ca}$  ( $\sim 38$  percent), and  $^{45}\text{K}$  ( $\sim 17$  percent) with its principal sources as  $^{36}\text{Ar}$  ( $\sim 64$  percent) and  $^{40}\text{Ca}$  ( $\sim 19$  percent). The  $^{36}\text{Ar}$  is converted into  $^{45}\text{Sc}$  by  $(p, n)$  reactions on the  $^{45}\text{Ca}$  made in the sequences described under  $^{46}\text{Ca}$  production. The  $(n, \gamma)$  and  $(p, n)$  cross-sections of  $^{45}\text{Ca}$  seem rather important, therefore.

f)  $^{47}\text{Ti}$ ,  $^{49}\text{Ti}$ ,  $^{50}\text{Ti}$ , and  $^{50}\text{V}$

The synthesis of these four nuclei is closely associated with that of  $^{48}\text{Ca}$ . The  $^{47}\text{Ti}$  is produced as  $^{47}\text{Ti}$  ( $\sim 13$  percent),  $^{47}\text{Sc}$  ( $\sim 34$  percent),  $^{47}\text{Ca}$  ( $\sim 37$  percent), and  $^{47}\text{K}$  ( $\sim 16$  percent), with its principal sources being  $^{40}\text{Ca}$  ( $\sim 45$  percent),  $^{36}\text{Ar}$  ( $\sim 34$  percent), and  $^{38}\text{Ar}$  ( $\sim 17$  percent). The  $^{40}\text{Ca}$  and  $^{38}\text{Ar}$  seed contribute through the reaction sequence  $^{40}\text{Ca}(n, \gamma)^{41}\text{Ca}(n, \alpha)^{38}\text{Ar}(n, \gamma) \dots ^{44}\text{Ar}(p, n)^{44}\text{K}(n, \gamma) \dots ^{47}\text{K}(p, n)^{47}\text{Ca}(p, n)^{47}\text{Sc}(p, n)^{47}\text{Ti}$ , and the  $^{36}\text{Ar}$  seed nuclei contribute by the sequence  $^{36}\text{Ar}(n, \gamma)^{37}\text{Ar}(n, p)^{37}\text{Cl}(n, \gamma) \dots ^{45}\text{Cl}(p, n)^{45}\text{Ar}(n, \gamma)^{46}\text{Ar}(p, n)^{46}\text{K}(p, \gamma)^{47}\text{Ca}(p, n)^{47}\text{Sc}(p, n)^{47}\text{Ti}$ . The reactions  $^{41}\text{Ca}(n, \alpha)^{38}\text{Ar}$ , and  $^{37}\text{Ar}(n, p)^{37}\text{Cl}$  and  $(p, n)$  reactions, especially at  $A = 47$ , again play the dominant role.

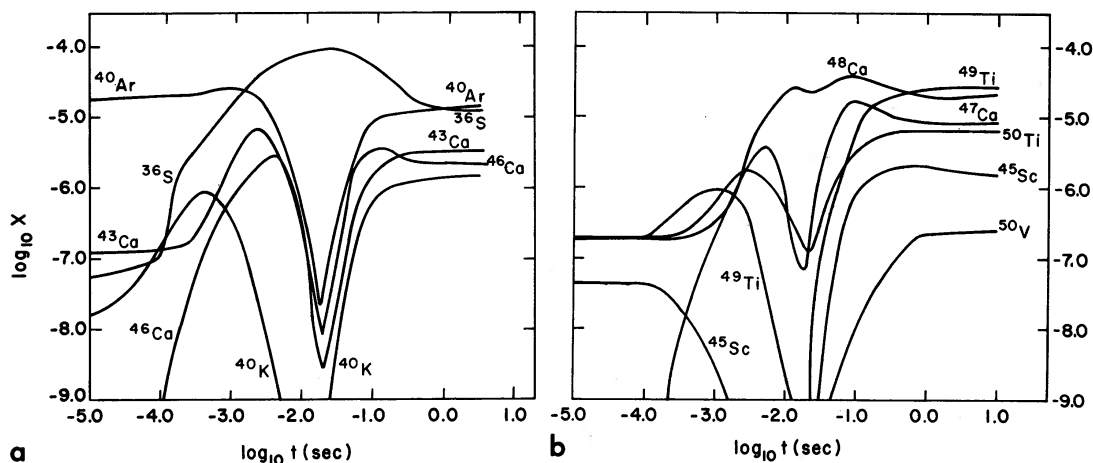


FIG. 3.—(a) and (b). The abundances of important nuclei are shown as a function of time during the burning at  $T_9 = 2.15$ . The abundances of those nuclei due to  $(p, n)$  and  $(p, \gamma)$  reactions ( $^{40}\text{Ar}$ ,  $^{40}\text{K}$ ,  $^{43}\text{Ca}$ ,  $^{46}\text{Ca}$ ,  $^{45}\text{Sc}$ ,  $^{47}\text{Ca}$ ,  $^{49}\text{Ti}$ ,  $^{50}\text{Ti}$ , and  $^{50}\text{V}$ ) increase very rapidly between  $10^{-2}$  and  $10^{-1}$  s, while the abundances of those nuclei due to neutron induced reactions ( $^{36}\text{S}$  and  $^{48}\text{Ca}$ ) are somewhat reduced during this time. See details in text.



The  $^{49}\text{Ti}$  is produced as  $^{49}\text{Ti}$  ( $\sim 50$  percent) and  $^{49}\text{Sc}$  ( $\sim 50$  percent) with the sources  $^{40}\text{Ca}$  ( $\sim 63$  percent),  $^{36}\text{Ar}$  ( $\sim 16$  percent), and  $^{38}\text{Ar}$  ( $\sim 15$  percent). The  $^{49}\text{Ti}$  is produced in the proton phase from the following continuation of the above-mentioned reaction sequences:  $^{47}\text{Ca}(n, \gamma)^{48}\text{Ca}(p, \gamma)^{49}\text{Sc}(p, n)^{49}\text{Ti}$ , and  $^{47}\text{Ca}(p, n)^{47}\text{Sc}(n, \gamma)^{48}\text{Sc}(n, \gamma)^{49}\text{Sc}(p, n)^{49}\text{Ti}$ .

The  $^{50}\text{Ti}$  is produced as  $^{50}\text{Ti}$  ( $\sim 58$  percent) and  $^{50}\text{Sc}$  ( $\sim 42$  percent) and also has as its sources  $^{40}\text{Ca}$  ( $\sim 75$  percent),  $^{36}\text{Ar}$  ( $\sim 9$  percent), and  $^{38}\text{Ar}$  ( $\sim 9$  percent) through the following reactions on  $^{49}\text{Sc}$ :  $^{49}\text{Sc}(p, n)^{49}\text{Ti}(n, \gamma)^{50}\text{Ti}$  and  $^{49}\text{Sc}(n, \gamma)^{50}\text{Sc}(p, n)^{50}\text{Ti}$ .

The nucleus  $^{50}\text{V}$  is essentially stable, having a half-life  $\tau_{1/2} = 6 \times 10^{15}$  years, and is surrounded by the stable isobars  $^{50}\text{Cr}$  and  $^{50}\text{Ti}$ . In this calculation we produce the  $^{50}\text{V}$  from  $^{40}\text{Ca}$  ( $\sim 61$  percent),  $^{36}\text{Ar}$  ( $\sim 18$  percent), and  $^{38}\text{Ar}$  ( $\sim 15$  percent) by the reaction sequences  $^{49}\text{Ti}(p, n)^{49}\text{V}(n, \gamma)^{50}\text{V}$  and  $^{49}\text{Ti}(p, \gamma)^{50}\text{V}$ . The  $^{50}\text{V}$  is easily destroyed during the burning by  $^{50}\text{V}(n, p)^{50}\text{Ti}$ .

It will be clear that each of the reactions mentioned is of some importance and that careful nuclear measurements are needed.

g)  $^{62}\text{Ni}$ ,  $^{64}\text{Ni}$ ,  $^{68}\text{Zn}$ ,  $^{70}\text{Zn}$ , and  $^{76}\text{Se}$

Because of the large abundances just beyond Cr, the capture by Cr seed did not enrich significantly the natural abundance of any nucleus. Of special interest (Peters *et al.* 1972) is the fact that  $^{54}\text{Cr}$  definitely does not owe its abundance to such events as described here.

The neutron cross-sections in Ni and Fe are large enough that the seed is quickly driven out to more massive isotopes until it is stopped by  $(\gamma, n)$  reactions on an isotope that has a low ( $\sim 4.5$ – $5.0$  MeV) neutron separation energy. The situation resembles the traditional picture of the  $r$ -process (Burbidge *et al.* 1957; Seeger, Fowler, and Clayton 1965; Clayton 1968) except that there is insufficient time for  $\beta$ -decays to allow the flow to continue and the flow terminated at the waiting point. The effect of  $(p, n)$  reactions can be ignored for the establishment of the isotopic equilibrium, although they play the role of the  $\beta$ -decays. The flow in Ni is halted at  $^{68}\text{Ni}$  and  $^{70}\text{Ni}$  because an equilibrium is established between  $(n, \gamma)$  and  $(\gamma, n)$  reactions between  $^{68}\text{Ni}$  and  $^{69}\text{Ni}$  and between  $^{70}\text{Ni}$  and  $^{71}\text{Ni}$ . These equilibria are established because of the low neutron separation energies of  $^{69}\text{Ni}$  and  $^{71}\text{Ni}$ , which are not experimentally determined. After the explosive ejection,  $^{68}\text{Ni}$  and  $^{70}\text{Ni}$  decay to  $^{68}\text{Zn}$  and  $^{70}\text{Zn}$ , and we see in table 2 that the solar abundances of  $^{68}\text{Zn}$  and  $^{70}\text{Zn}$  are well accounted for if such zones are responsible for all of the production of  $^{24}\text{Mg}$ .

A similar situation occurs for Fe. The neutron flow is halted at  $^{62}\text{Fe}$  and  $^{64}\text{Fe}$  because of the low neutron separation energies of  $^{63}\text{Fe}$  and  $^{65}\text{Fe}$ , which are also not experimentally determined. After the explosive ejection the  $^{62}\text{Fe}$  and  $^{64}\text{Fe}$  decay to  $^{62}\text{Ni}$  and  $^{64}\text{Ni}$  in amounts roughly sufficient to account for their natural abundances.

The next even- $Z$  element, zinc, is driven to  $^{76}\text{Zn}$ , from which it decays to  $^{76}\text{Se}$  after the event with approximately the proper yield, as shown in table 2.

These seem to be the only elements in which the element abundance exceeds by two orders of magnitude the abundance of the waiting-point isobar. Thus, for example, the heavy  $r$ -process nuclei discussed by Seeger *et al.* (1965) are definitely not due to events like those described here. The values of the neutron-capture cross-sections matter very little in these calculations. It is the neutron separation energies that matter. It seems to us that a great opportunity exists here, because the relative yields of these five nuclei depend almost entirely on only a few separation energies for nuclei that are not hopelessly far removed from the valley of beta stability, as they are in the conventional  $r$ -process. The spins of low-lying states of neutron-rich nuclei also play a role in their contribution to the nuclear partition functions. Consider the example of  $^{63}\text{Fe}$  in equi-

librium with  $^{62}\text{Fe}$  and neutrons:

$$\frac{N(^{63}\text{Fe})}{N(^{62}\text{Fe})} \propto N_n \frac{\omega(^{63}\text{Fe})}{\omega(^{62}\text{Fe})} \exp \left[ -\frac{S_n(^{63}\text{Fe})}{kT} \right].$$

The value of this ratio is very important because the  $^{63}\text{Fe}$  concentration determines the  $(n, \gamma)$  flow that is able to penetrate onward to  $^{64}\text{Fe}$ . Although the  $^{63}\text{Fe}$  concentration is negligible insofar as synthesis of nuclei at  $A = 63$  is concerned, it does moderate the  $^{62}\text{Fe}/^{64}\text{Fe}$  ratio and, thereby, the  $^{62}\text{Ni}/^{64}\text{Ni}$  yield. What the formula reminds us is that the separation energy of a neutron from  $^{63}\text{Fe}$  and the statistical weight  $\omega(^{63}\text{Fe}) = \sum E_i (2J_i + 1) \exp(-E_i/kT)$  of the  $^{63}\text{Fe}$  nucleus, as reflected by the spins  $J_i$  and excitations  $E_i$  of its quantum states, enter in important ways into this calculation. Reliable nuclear information will thus place very tight constraints on the explosions capable of satisfying the solar  $^{62}\text{Ni}/^{64}\text{Ni}$  abundance ratio.

However, it may be that  $^{62}\text{Ni}$  is synthesized in an  $e$ -process followed by an alpha-rich freezeout (Arnett, Truran, and Woosley 1971), which successfully and convincingly coproduces  $^{60,61,62}\text{Ni}$ . Its success would suggest that  $^{62}\text{Ni}$  should not be synthesized from seed nuclei as in this paper. On the other hand, one must put the Fe seed nuclei somewhere. If about  $1/200 \text{ g g}^{-1}$  of matter have passed through explosive carbon burning, as is suggested by the coproduction of  $^{20}\text{Ne}$ ,  $^{23}\text{Na}$ ,  $^{24,25,26}\text{Mg}$ , and  $^{27}\text{Al}$ , then  $1/200$  of the iron mass fraction must appear as neutron-rich isotopes. Only  $^{60}\text{Ni}$  and  $^{62}\text{Ni}$  are capable of absorbing this mass ( $\sim 5 \times 10^{-6} \text{ g g}^{-1}$ ); and it does not appear, from our calculations, that the  $(n, \gamma)$  flow in Fe can possibly stop at  $^{60}\text{Fe}$  in explosive carbon burning. Thus if we take the position that  $^{62}\text{Ni}$  is not produced from seed nuclei as we have described, we are led to ask, "Where does the Fe seed go?" There is no abundance capable of hiding it. It will probably be some time before this problem is correctly unraveled, but this calculation certainly illuminates the problem.

#### *h) $^{65}\text{Cu}$ , $^{67}\text{Zn}$ , $^{69}\text{Ga}$ , $^{73}\text{Ga}$ , $^{73}\text{Ge}$ , and $^{75}\text{As}$*

The odd- $Z$  nuclei do not have sufficiently large abundances to form seed for nucleosynthesis. If, on the other hand, of order 10 percent of Fe and Ni undergo  $(p, n)$  reactions while held up at their waiting points, the resultant production of Co and Cu isotopes is sufficient to allow synthesis of the nuclei listed above. The Co flow waits at  $^{65}\text{Co}$  and  $^{67}\text{Co}$ , with their relative abundances determined largely by the unknown  $^{66}\text{Co}$  neutron separation energy. The Cu isotopes distribute themselves at  $A = 69, 71, 73$ , and  $75$  in rather uncertain abundance ratios because of the uncertain neutron separation energies.

We calculated  $(p, n)$  cross-sections for Fe and Ni isotopes with the optical model approach described by Michaud and Fowler (1970), and our results were included in table 1. The fraction of nickel undergoing  $(p, n)$  transmutation, for example, drops from 27 percent to 1 percent as  $T_9$  drops from 2.15 to 2.00. As a result, we see in table 2 that the odd- $A$  overabundances show a strong temperature dependence. If we are to have these nuclei coproduced in this way, our results suggest that explosive carbon burning occurs primarily at temperatures less than  $T_9 = 2.15$  but at least as great at  $T_9 = 2.0$ . It is interesting that the final yields of the primary products suggest the same conclusion. For the final yields of these nuclei we shall need good estimates of the  $(p, n)$  cross-section of  $^{62,64}\text{Fe}$ ,  $^{68,70}\text{Ni}$ ,  $^{65,67}\text{Co}$ , and  $^{69,71,73,75}\text{Cu}$ , as well as good estimates of the relevant neutron separation energies and nuclear statistical weights.

A preliminary account of this investigation has already been published (Howard *et al.* 1971). Subsequent recalculation of the  $(p, n)$  rates on neutron-rich isotopes of Fe and Ni indicated somewhat larger cross-sections than the estimates we used for that preliminary report. The reader will note some differences in the earlier table from the  $T_9 = 2.15$

column of table 2 due to these recalculations. The larger  $(p, n)$  cross-sections used in this paper cause larger overabundances of the odd- $A$  heavy nuclei.

It is natural to wonder if this combination of  $(p, n)$  and  $(n, \gamma)$  chains cannot account for even more massive  $r$ -process nuclei. We doubt it for explosive carbon burning, although there may be other contexts in which the combination might also work quite naturally. The seed/product ratio becomes much smaller at larger atomic weights.

#### V. DISCUSSION

These calculations have rested on a system we call the "perturbation method": the free nucleon densities are computed separately from a carbon-burning network as in Arnett (1969), and these densities are then used to calculate the abundance alteration of heavier nuclei. We assume that the existence of the heavier nuclei has not invalidated the free-nucleon densities. It is reasonable to now examine the validity of this approach. The heavy nuclei ( $Z \geq 16$ ) started with an initial mass fraction  $X_{\text{initial}}^{\text{seed}} = 2.14 \times 10^{-3}$  and initial neutron excess per nucleon  $\eta_{\text{initial}}^{\text{seed}} \equiv (N - Z)/(N + Z) = 5.0 \times 10^{-2}$  and evolved to final quantities  $X_{\text{final}}^{\text{seed}} = 2.31 \times 10^{-3}$  and  $\eta_{\text{final}}^{\text{seed}} = 13.9 \times 10^{-2}$ . The changes are largely due to the capture of free neutrons and are dominated by the iron seed. The density of excess neutrons in the primary material is  $\eta = 2 \times 10^{-3}$  g of neutrons per gram of matter, located in our calculation in  $^{18}\text{O}$ , whereas the density of neutrons captured by heavy seed is only  $X^{\text{seed}} \Delta\eta^{\text{seed}} = (2.3 \times 10^{-3})(8.9 \times 10^{-2}) = 2.0 \times 10^{-4}$  g of neutrons per gram of matter. Thus the basic carbon-burning network loses about 10 percent of its excess neutrons to the seed nuclei, suggesting that their explicit inclusion in the basic program (unfortunately prohibitive) would have reduced the free-neutron density by the order of 10 percent. We actually confirmed this result by including a single neutron-capturing seed nucleus in the basic program. Thus this aspect of the perturbation concept is satisfactory. As far as the basic carbon-burning program is concerned, one need only take into account that its  $\eta$  is effectively reduced 10 percent (at all three temperatures) by the seed nuclei. Because these neutrons are captured early in the burning, the basic carbon-burning program can be accurately doctored by inclusion of a single dummy seed nucleus (for convenience,  $^{56}\text{Fe}$ ) at a mass fraction  $X(\text{Fe}) = 2.2 \times 10^{-3}$  and allowing that nucleus to capture six neutrons per seed nucleus with a cross-section near 10 millibarns, after which its  $(n, \gamma)$  cross-section is set equal to zero. This approximation is sufficiently accurate. The proton absorption by the seed nuclei can be neglected altogether in the generation of the free-proton density.

The approximation that the seed nuclear interactions can be decoupled from the carbon burning begins to break down at the temperature  $T_9 = 2.15$  for a different reason. The final  $^{32}\text{S}$  abundance, which is a steeply rising function of the burning temperature, was 6 times its initial seed abundance after this carbon-burning calculation. However, the  $^{32}\text{S}$  is being produced near  $t \simeq 6.0 \times 10^{-2}$  s when the neutrons are beginning to be exhausted. We expect the growing  $^{32}\text{S}$  to provide an increased contribution from  $^{32}\text{S}$  seed to  $^{36}\text{S}$ ,  $^{40}\text{Ar}$ , and  $^{40}\text{K}$  by no more than a factor 3. This results in a total increase in the yield of  $^{36}\text{S}$  by a factor 2 and less for  $^{40}\text{Ar}$  and  $^{40}\text{K}$ . We feel that this uncertainty is no more significant than the uncertainties introduced by lack of nuclear data, although this is the highest temperature at which we feel the perturbation approach as we have done it is applicable. At  $T_9 \geq 2.15$  it would be preferable to enlarge the carbon-burning network to include S-Cl-Ar isotopes.

We have presented only a limited survey of the possibilities. Significant alterations of the free-nucleon densities are possible within the basic program by (1) altering the density; (2) altering the hydrodynamic timescale; (3) altering the initial composition, e.g.  $X(^{12}\text{C})$ ,  $X(^{18}\text{O})$ ,  $X(^{22}\text{Ne})$ , etc.; and (4) altering the major reaction rates governing the free-nucleon densities. These effects should first be explored within the basic survey of carbon burning, rather than in the heavy-seed problem, and it seems sensible to await more thorough descriptions of the hydrodynamics of exploding carbon shells of stars.

We must acknowledge that these calculations we have presented only scratch the surface of a difficult problem. Our results *are* promising and suggest that, with adequate nuclear information, severe constraints could be placed on the explosive circumstances.

In this whole system there exists a challenge for laboratory nuclear astrophysics. Only careful measurements of key nuclear facts can clarify the correctness of the hypothesis. Basic to these are the cross-sections. To emphasize this we included in table 1 and in its footnotes the symbol \* after each important reaction rate and the symbol \*! after those of the highest importance to this problem. We urge those engaged in laboratory nuclear astrophysics to consider which of these reactions they can investigate by measurements or nuclear theory. Also needed are the neutron separation energies and statistical weights of neutron-rich nuclei. This problem is not new. It has existed since the *r*-process was formulated. But the information needed for this problem is for nuclei close to the mass valley of stability. Unless nuclear facts disprove this scheme, it seems likely that it can explain the origins of many of the rare nuclear species.

We wish to thank W. A. Fowler, G. Michaud, and J. W. Truran for many helpful discussions relevant to this problem. The computations were carried out with a generous gift of time on the IBM 360-44 of the Institute of Theoretical Astronomy. This research was also supported in part by the National Science Foundation under grants GP-18335 and GP-23459.

#### REFERENCES

- Allen, B. J., Gibbons, J. H., and Macklin, R. L. 1971, in *Advances in Nuclear Physics*, Vol. 4, ed. M. Baranger and E. Vogt (New York: Plenum Press), p. 205.
- Arnett, W. D. 1969, *Ap. J.*, **157**, 1369.
- Arnett, W. D., and Clayton, D. D. 1970, *Nature*, **227**, 1.
- Arnett, W. D., and Truran, J. W. 1969, *Ap. J.*, **157**, 339.
- Arnett, W. D., Truran, J. W., and Woosley, S. E. 1971, *Ap. J.*, **165**, 87.
- Bodansky, D., Clayton, D. D., and Fowler, W. A. 1968, *Ap. J., Suppl.*, **16**, 299.
- Burbidge, E. M., Burbidge, G. R., Fowler, W. A., and Hoyle, F. 1957, *Rev. Mod. Phys.*, **29**, 547.
- Cameron, A. G. W. 1968, in *The Origin and Distribution of the Elements*, ed. L. H. Ahrens (New York: Pergamon Press), p. 125.
- Clayton, D. D. 1968, *Principles of Stellar Evolution and Nucleosynthesis* (New York: McGraw-Hill Book Co.), chap. 7.
- Eberhardt, P. J., Geiss, J., Graf, H., Grögler, N., Krähenbühl, U., Schwaller, H., Schworzmüller, J., and Stettler, A. 1970, preprint submitted to *Geochim. Cosmochim. Acta*.
- Fowler, W. A., Caughlan, G. R., and Zimmerman, B. A. 1971, private communication; see also *Ann. Rev. Astr. and Ap.*, **5**, 525 (1967).
- Garvey, G. T., Gerace, W. J., Jaffe, R. L., Talmi, I., and Kelson, I. 1969, *Rev. Mod. Phys.*, **41**, S1.
- Howard, W. M., Arnett, W. D., Clayton, D. D., and Woosley, S. E. 1971, *Phys. Rev. Letters*, **27**, 1607.
- Mattauch, J. H. E., Thiele, W., Wapstra, A. H. 1965, *Nucl. Phys.*, **67**, 1.
- Michaud, G., and Fowler, W. A. 1970, *Phys. Rev. C*, **2**, 2041.
- Peters, J., Fowler, W. A., and Clayton, D. D. 1972, submitted to *Ap. J.*
- Seeger, P. A., Fowler, W. A., and Clayton, D. D. 1965, *Ap. J. Suppl.*, No. 97, 11, 121.
- Truran, J. W. 1971, private communication; see also *Ap. and Space Sci.*, **2**, 384 and 391 (1968).
- Truran, J. W., and Arnett, W. D. 1970, *Ap. J.*, **160**, 181.
- Woosley, S. E., Arnett, W. D., and Clayton, D. D. 1972, in preparation for *Ap. J. Suppl.*